444 *Macromolecules* **2011**, *44*, 444–452
DOI: 10.1021/ma102371d

Macromolecules
ARTICLE

General Avenue to Individually Dispersed Graphene Oxide-Based Two-Dimensional Molecular Brushes by Free Radical Polymerization

Lanyan Kan, Zhen Xu, and Chao Gao*

MOE Key Laboratory of Macromolecular Synthesis and Functionalization, Department of Polymer Science and Engineering, Zhejiang University, 38 Zheda Road, Hangzhou 310027, P. R. China

Received August 25, 2010; Revised Manuscript Received December 19, 2010

ABSTRACT: We present a general strategy for facile synthesis of 2D macromolecular brushes. The ultraflat one-atomic layer of graphene oxide with micrometer-scale sheet topology was employed as the macromolecular backbone; more than 10 types of polymer chains were covalently tethered to the nanosheets through free radical polymerization, producing various 2D molecular brushes with multifunctional arms covering from polar to apolar, water-soluble to oil-soluble, acidic to basic, and functional to common polymers. The resulting molecular brushes are well soluble in desired solvents in the forms of individually dispersed hairy nanosheets. The growing process of 2D molecular brushes was clearly visualized by AFM. The giant 2D brushes with arm density up to 1.59×10^4 arms per μm^2 of single side of graphene show high solubility (~15 mg/mL), low intrinsic viscosity (~100 mL/g), and fine electrical conductivity ($\sim 8.4 \times 10^{-3}$ S/cm), and they can possess numerous epoxy and other functional groups at their arms if necessary, promising a luciferous foreground in both scientific research and industrial applications. The polymer-grafted graphene oxide can be well dispersed in free polymer matrix and can be well soluble in solvents again, suggesting that nanocomposite of polymer-grafted graphene oxide and polymer can be readily produced by the solution-processing technique.

Introduction

Attaching high-density polymeric chains/arms with one end to a macromolecular backbone or a solid substrate affords a molecular polymer brush or a surface polymer brush. Interest in molecular brushes began more than 30 years ago for their unique structure and biomimetic applications such as water-based lubrication.[1−5] One-dimensional (1D) cylindrical molecular brushes have been widely addressed,[6,7] and cyclic brushes were also successfully synthesized in 2008 by Deffieux and co-workers.[8] Recently, surface brushes have been also prominently advanced with the utilization of controlled radical polymerization (CRP) techniques.[9−12] In this respect, 2D surface brushes are of particular interest because of their unusual stimuli-responsive properties and potential applications to stabilize colloids, reduce friction between surfaces, and provide lubrication in artificial joints.[13−16] However, the conventional 2D surface brushes are generally insoluble in solvents, posing a big barrier for their solution-based processing, and it is almost impossible to directly grow polymer brushes on a target surface in the practical applications. Hence, to construct 2D molecular brushes, annexing the features of good solubility of linear molecular brushes and flat-topology of 2D surface brushes becomes a dream for both scientists and engineers.

The synthesis of 2D molecular brushes seems to be a big challenge for chemists owing to the absence of both efficient methodology and active 2D molecular backbone even though the theoretical calculations of 2D molecular brushes had been reported.[17] Currently, the emergence of graphene[18−20] or graphene oxide[21−23] (GO) sheds a light on the accomplishment of such an object for its sheetlike structure. Although several groups had tried to graft polymer chains from/onto graphene/GO sheets via "grafting from", "grafting to", or *in situ* polycondensation approach,[24−29] no one approached the target of 2D molecular bushes intentionally. Three reasons are likely responsible for this situation. First, all of the reports focused their attention on the functionalization of graphene or GO for improving their solubility, whereas neglected that graphene or GO themselves are perfect candidates of 2D *macromolecular* backbone for 2D molecular brushes. As a consequence, polymer-grafted graphene or polymer-grafted GO hybrids are commonly applied as fillers to improve the mechanical properties of polymer composites due to their good compatibility and enhanced interfacial interactions, and they are never regarded as *macromolecules*, not to mention their molecular intrinsic characters such as viscosity. Second, the oxygen-contained functional groups of GO are mainly employed as grafting sites, usually leading to uneven and unstable grafting as well as strong aggregation because such groups are mostly located at the sheet edges and are easily decomposed during reaction.[30,31] Hence, individually dispersed sheet brushes demonstrated by distinct observations of AFM are rarely achieved. Notably, the aggregated compounds cannot be regarded as *molecular* brushes anymore but *nonmolecular* matter or the conventional surface/solid brushes from a strict point of view. Third, no general and facile methodology is presented. Although CRP techniques such as atom transfer radical polymerization (ATRP) had been used to graft specific polymer chains on graphene or GO surfaces, no one developed a general approach that is compatible to construct 2D molecular brushes with the three common classes of vinyl monomers of (meth)acrylates, styrenes, and acrylamides. Besides, it needs extra steps to introduce initiating groups on graphene or GO sheets before polymer grafting for CRP, so the procedure is relatively complex. More seriously, the multistep reactions raise the risk of their aggregation, which is adverse for the target of individually dispersible

*To whom correspondence should be addressed. E-mail: chaogao@zju.edu.cn.

 Published on Web 12/31/2010

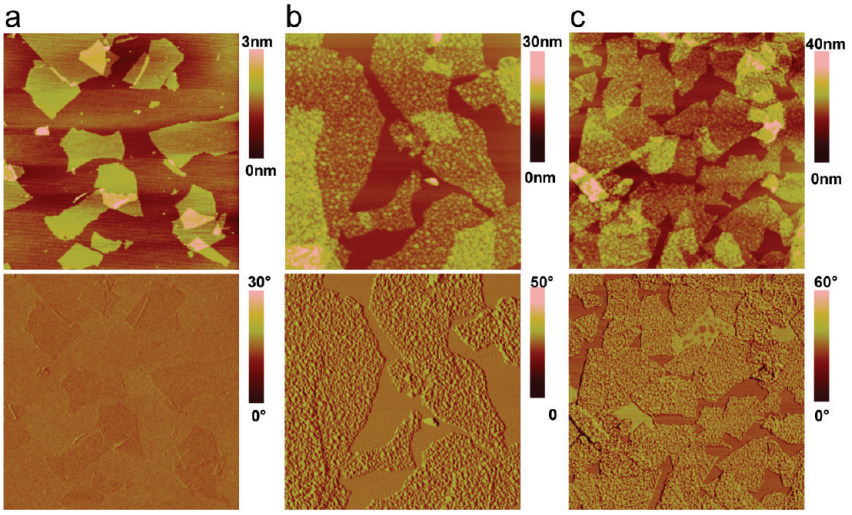

Figure 1. (a) Height (above) and phase (below) images of GO with size of 5 μm × 5 μm. (b, c) Height (above) and phase (below) images of the resultant GO-*g*-PGMA two-dimensional macromolecular brushes with molar feed ratios of monomer to initiator 50:1 (b) and 200:1 (c), with reaction time of 7.5 and 48 h and the sizes of 2.5 μm × 2.5 μm and 5 μm × 5 μm, respectively.

2D molecular brushes. Accordingly, effective synthesis of molecular-level soluble 2D brushes is still to be resolved.

Here, we present a general, facile approach to 2D molecular brushes by conventional free radical polymerization (FRP) using graphene and GO nanosheets as flat *macromolecular* backbones. The widely used FRP can not only be simply operated but also be workable for almost all of vinyl monomers. The growing process of 2D molecular brushes were clearly visualized by AFM, showing that GO sheets maintain isolated with each other after polymer grafting. The resultant 2D molecular brushes show unique attributes such as low intrinsic viscosity, high solubility, good solution processability, and fine electrical conductivity, foretelling extensive applications and opening the new mine of 2D molecular brushes.

Experimental Section

Materials. Glycidyl methacrylate (GMA, Aldrich) and other vinyl monomers (Aldrich except the specially stated) were further purified by basic alumina column chromatography to remove the inhibitor. Sodium *p*-styrenesulfonate (PSSNa, Aladdin 90%) was used as received. 2,2′-Azobis-(2-methylpropionitrile) (AIBN) and potassium persulfate ($K_2S_2O_8$) were employed after twice recrystallization. Graphite powder (40 μm) was purchased from Qingdao Henglide Graphite Co. Ltd.

Instrumentation. AFM characterization was carried out on Nanoscope IIIa (Figures 1 and 2, Figures S1−S7, S11−S17, and S19) and NSK SPI3800 (Figure S9) under tapping mode. The samples were prepared by spin-coating onto freshly peeled mica wafer at 800 rpm from sample solutions. Thermal gravimetric analysis (TGA) was carried out using a Perkin-Elmer Pyris 6 TGA instrument with a heating rate of 20 °C/min under a nitrogen flow (30 mL/min). ^{1}H NMR spectra were obtained through the equipment of NMK/300 MHz. Fourier-transform infrared (FTIR) measurements were performed on a Bruker Vector 22 spectrometer (KBr disk). Scanning electron microscopy (SEM) images were carried on a Hitachi S4800 field-emission SEM system. Transmission electron microscopy (TEM) images were obtained through a XDT-10 electron microscope operating at 120 kV accelerating voltage. The X-ray diffraction (XRD) measurements were taken on a Philips X'Pert PRO diffractometer equipped with Cu Kα radiation (40 kV, 40 mA).

Synthesis of Two-Dimensional Macromolecular Brushes. Well-dispersed graphene oxide (GO) is synthesized from natural graphite powder using a modified Hummers method.[29,32,33] A typical polymerization procedure is given as follows: 50 mg of GO dispersed in 40 mL of *N*,*N*-dimethylformamide (DMF) was added to 100 mL Schlenk and sonicated in a 40 kHz sonic bath for 1 h followed by introducing 50 mmol of GMA monomer. Under N_2 flow protection and vigorous stirring, 0.25 mmol of AIBN was added. The Schlenk was then immersed in a 65 °C oil bath. After reacting for certain time (normally 48 h), the resultant solution was precipitated in methanol. The precipitates were collected and redissolved in 200 mL of DMF. The solution was transferred into centrifuge tubes (6 × 50 mL) and then centrifugated at the speed of 15 000 rpm (23 300*g*) for 0.5−1 h to collect the bottom black solids. This centrifugation was repeated (at least four times) until the upper layer was colorless. Then 200 mL of acetone instead of DMF was used to disperse the precipitates, and a similar centrifugation process was used and repeated (at least three times) to collect the resulting solid product. The product was dried in a vacuum oven at 35 °C for 12 h.

Results and Discussion

Strategy Design and Synthesis Exploring. To achieve 2D molecular brushes, the most important two key factors are the macromolecular backbone and the construction method. The backbone should possess sheet topology and multiple reactive sites. In this paper, we choose the macromolecules of graphene oxide (GO) or chemically reduced graphene as backbones. The micrometer-scale dimension of graphene nanosheets would make direct visualization of the resulting sheet brushes readily accessible, providing a direct approach to evaluate the effect of polymer grafting. As to the synthesis method, we select the common FRP to construct the 2D molecular brushes due to its simplicity and generality.

Previously, FRP had been successfully used to covalently graft polymer chains on carbon nanotubes (CNTs) by macromolecular radical addition to the reactive carbon−carbon double bonds,[34−38] casting a positive light for the polymer grafting on graphene oxide or graphene surface. Our synthesis strategy is illustrated in Scheme 1. Both of highly soluble graphene oxide (GO) and less soluble graphene were tested as backbones in our experiments. To avoid the possible aggregation of the backbones, polymer chains are directly attached to the sp^2-hybridized or double bonds of GO, rather than their functional groups that were commonly used in the

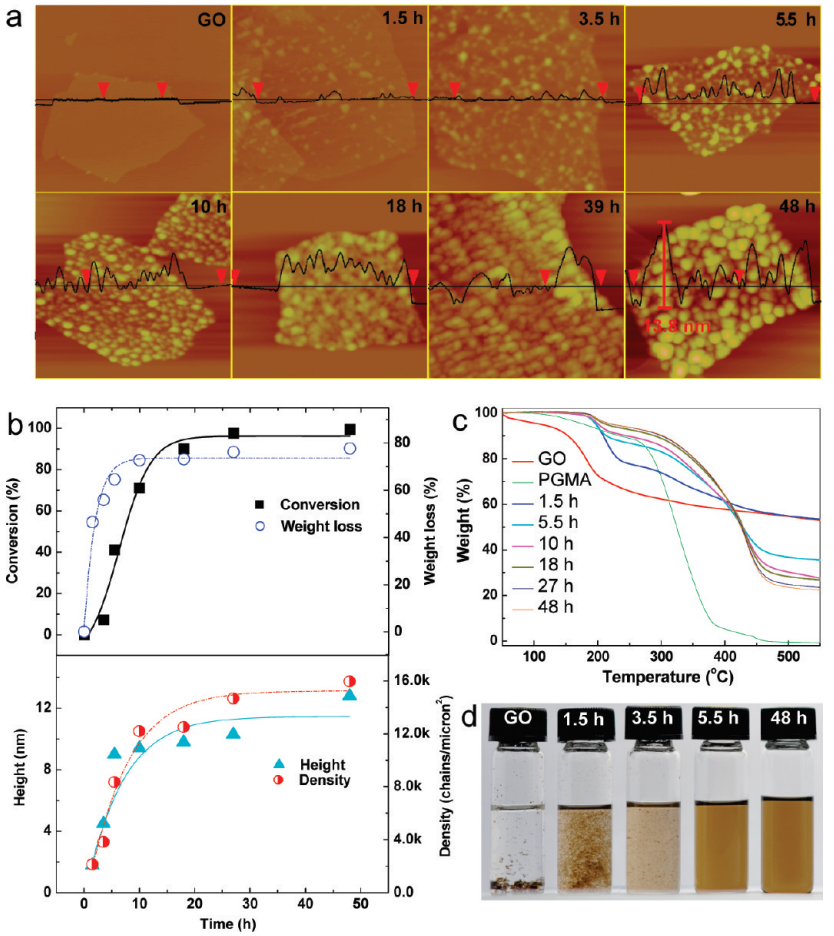

Figure 2. (a) AFM height images of GO and GO-*g*-PGMA 2D brushes at different reaction time (size for all images: 1 μm × 1 μm). (b) Conversion of monomer, TGA weight loss of brushes, the average height of polymeric arms on the 2D brushes, and the average density of polymeric arms as a function of reaction time. (c) TGA curves of GO, PGMA, and GO-*g*-PGMA brushes. (d) Photographs of GO and GO-*g*-PGMA brushes at different reaction time added into chloroform.

chemical modification.[31] After initiating of vinyl monomers by FRP, macromolecular radicals are formed immediately by chain propagation.[39] Part of the macromolecular radicals are added to double bonds of GO, producing graphene oxide-based brushes and simultaneously generating new radicals at its surface, which are then liable to further radical propagation, termination, or transfer. Notably, even though it is recognized that polymer chains can be directly grafted onto the graphitic surface by using such radical addition/coupling reaction between polymer radicals and the double bonds of surfaces, to provide the direct evidence for the detailed reaction mechanism is still an open question.

The macroradical coupling converts the sp^2 bonds into sp^3, which weakens the conjugacy of localized π-electron cloud and thus activates more sp^2 bonds nearby. It should be pointed out that many kinds of side reactions may happen during polymerization. For instance, V-shaped grafted polymers (when further chain propagation occurs on the same side of GO layer) and cyclic chains (when newly generated polymer radicals are subjected to coupling termination) would be formed. Resultantly, 2D molecular brushes with islands of arms would form.

To obtain molecular brushes with multifunctional reactive arms, we select GMA as the typical monomer to investigate the details. Figure 1 shows the AFM images of GO and poly(glycidyl methacrylate)-grafted GO (GO-*g*-PGMA). The original GO sheets spin-coated on a mica substrate are ultraflat indeed, with a thickness of 0.6−0.8 nm, indicating their single-layer atom structures.[40] For the two samples of GO-*g*-PGMA obtained at different polymerization conditions, various protuberances are observed on the sheet backbones with the average heights ($\bar{h}$) of 4.9 nm (Figure 1b) and 10.3 nm (Figure 1c), preliminarily demonstrating the success of polymer grafting. Significantly, the protuberances, tufts of polymeric hairs, are evenly distributed on the whole sheets, rather than just around their circumferences or edges that were usually figured as the highest reactive sites with the lowest steric hindrance, declaring the formation of 2D molecular brushes with relatively even arms. Lots of single hairy sheets are found in the view, implying the good dispersibility/solubility of the product and the reliability of the synthesis strategy. In addition, the sheet brushes showed the similar micrometer-scale dimension to the GO precursors, revealing the integrity of sheet backbones during the polymerization.

Brush Growth and Polymerization Kinetics. Besides the even grafting, another challenge is the controlled grafting on such a giant sheet, particularly upon the grafting density of arms. No one had ever tried to control the density of grafted polymers on both CNTs and GO yet, likely due to the difficulty of control over arm density through CRP. Herein, we attempt to resolve this problem by FRP kinetics, and thus we monitor the polymerization process by various techniques including AFM, nuclear magnetic resonance (NMR) spectroscopy, TGA, and gel permeation chromatography (GPC) characterizations.

Scheme 1. Synthesis of 2D Macromolecular Brushes by Free Radical Polymerization of Various Monomers with the Backbone of GO Sheets[a]

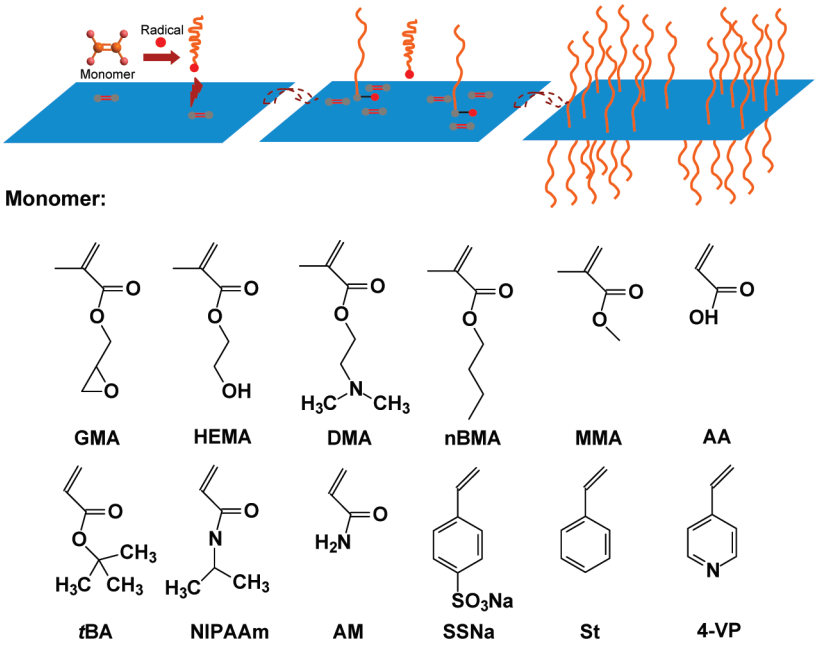

[a] The blue sheet represents GO, and the red dots and double bonds represent radicals and active grafting points, respectively.

Table 1. Selected Results of GO-*g*-PGMA 2D Macromolecular Brushes at Different Polymerization Time

reaction time (h)	average height (nm)[a]	weight loss (%)[b]	$\overline{d}_1$ (chains/10^4 carbon)[c]	$\overline{d}_2$ (chains/μm^2)[d]
1.5	1.8	46.5	1.1	2140
3.5	4.5	55.9	2.0	3830
5.5	9.0	64.6	4.4	8360
10	9.4	72.7	6.4	12200
18	9.8	73.2	6.6	12510
27	10.3	76.2	7.7	14670
48	12.8	77.7	8.4	15960

[a] Average height of polymer clusters on GO surfaces obtained from corresponding AFM images. [b] Weight loss in TGA curves below 550 °C. [c] Average density of the grafted polymer chains on GO with the unit of chains per 10^4 carbon atoms calculated from eq 2. For the samples above 3.5 h, W_P is the weight loss of brushes listed in the table because of the sharp increasing of grafted PGMA amount as well as partial reduction of GO backbone; for the samples at 1.5 and 3.5 h, W_P is equal to the total weight loss of brushes below 550 °C by subtracting the weight loss of unstable functional groups on GO backbone below 250 °C (i.e., 21.46 and 19.04 wt % for the two samples, respectively). [d] Average density of the grafted polymer chains on a single side of GO with the unit of chains per μm^2 calculated from eq 4.

AFM is found to be the most powerful tool for the visualization of graphene, GO sheets, and 2D molecular brushes. Figure 2a shows the kinetic AFM images of brushes traced at different polymerization time (see also Figures S1−S7). The pristine GO sheet is clean and smooth. After polymerization, bundles of hairy polymers are grafted on the sheet backbone. The cross-sectional view of kinetic AFM images indicates that the height and density of hairy polymers increased with the polymerization time. Obviously, at 1.5 h, sparsely isolated clusters of polymers are observed with the average height ($\overline{h}$) 1.8 nm; at 3.5 h, part of hairy islands are connected with $\overline{h}$ 4.5 nm; at 5.5 h, most of islands are merged into bigger ones with $\overline{h}$ 9.0 nm; at 10 h, the hairy clusters join together with $\overline{h}$ 9.4 nm and only a little of vacancy can be found on the sheet; after 18 h, continual hairy phase appear with the morphology of fused polymer clusters, and the $\overline{h}$ increases from 9.8 nm at 18 h to 11.3 nm at 39 h and 12.8 nm at 48 h (Table 1). From the AFM images, we can find that $\overline{h}$ increases with increasing the average grafting density ($\overline{d}$) of brushes. So the $\overline{d}$ and $\overline{h}$ of 2D molecular brushes can be tuned to some extent through the reaction time, which is favorable to the design, production, and application of the brushes-based devices, materials, and bio-nanoconjugates.

The kinetic samples were also characterized by ^{1}H NMR, GPC, and TGA measurements. ^{1}H NMR spectra (Figure S8) revealed that the polymerization in the presence of GO followed the typical kinetics rule of FRP:[39] the monomer conversion increased slowly at the initial 3.5 h with the conversion below 10%, rapidly within 18 h, and then very slowly after 25 h with the conversion above 90%, as shown in Figure 2b. In addition, the kinetics of GMA polymerization in the absence of GO was also investigated (Figure S9). It can be found that the polymerization of GMA in pure DMF solution was slightly quicker than that in GO dispersion. Nevertheless, the polymerization processes in two situations displayed a parallel trend. A similar phenomenon was also observed for other substrate-based polymerizations including CNT-based "grafting from" cases.[41] This is likely caused by the influence of the substrates on the monomer/initiators movements. The detailed reason is still an open question awaited for further investigations.

GPC results showed that the number-average molecular weight (M_n) of free polymers undulated around 5×10^4 g/mol after 5.5 h (see Table S1 and Figure S10), also being in agreement with the rule of molar mass variation for FRP.

Figure 2c shows the weight loss curves of GO and resulting brushes. There is an obvious weight loss stage (~36 wt %) for GO below 250 °C, which is assigned to the decomposition of oxygen-contained groups of GO.[42] For polymer-grafted GO

samples, two weight loss stages at 200−250 and 250−550 °C are observed. The first stage below 250 °C is resulted from the decompositions of unstable groups of GO as well as small part of grafted PGMA (see the neat PGMA curve for comparison); another stage above 250 °C belongs to the main decomposition of grafted PGMA. For the brushes obtained after 5.5 h of polymerization, the weight loss proportion below 250 °C is quite low, indicating that GO was partially reduced (see also XRD patterns for further evidence, Figure S11) and the labile groups in GO were degraded during the polymerization. Accordingly, all of the weight loss below 550 °C for the brushes after 5.5 h can be ascribed to the pyrolysis of grafted PGMA. We also clearly find that the amount of grafted polymers displays a similar rising tendency to the monomer conversion upon reaction time (Figure 2b). Notably, control experiments demonstrated that the ungrafted polymer can be efficiently removed by repeated washing (Figure S12). So, the measured polymer content by TGA is that of polymeric arms covalently grafted on GO backbone. Incidentally, the decomposition temperatures of grafted arms are increased by 30−55 °C (Figure 2c) and the glass transition temperatures enhanced about 7 °C[43] (Figure S13) as compared to the free polymers, revealing the role of free radical scavenger for GO and the confined chain movement for the anchored polymers.

The solubility of 2D brushes also increases with the reaction time: GO is totally insoluble and dispersible in chloroform, budding brushes at 1.5 h are dispersible as big conglomerates, part of brushes at 3.5 h are soluble accompanying with some small solid clusters, and all of brushes are well soluble after 5.5 h of polymerization (Figure 2d). These results demonstrate that the content and density of grafted polymer arms can be varied in a relatively wide range through polymerization time or monomer conversion.

Quantitatively, the $\bar{d}$ of 2D brushes (chains per 10^4 carbon atoms in GO, $\bar{d}_1$) can be calculated from the equation[44]

$$\bar{d}_1 = \frac{M_C}{M_P}\frac{W_P}{W_C} \times 10^4 \quad (1)$$

where M_C means the relative molar mass of carbon (M_C = 12), M_P the average molecular weight of grafted polymer (in this article, we assume that the grafted polymer has a comparable molecular weight to the free polymer, so $M_P = 5 \times 10^4$ is used for rough estimation of arm density), and W_C and W_P the weight fractions of graphene oxide backbone and grafted polymer, respectively. Since M_C and M_P are constants herein, eq 1 is simplified as

$$\bar{d}_1 = K_1\frac{W_P}{W_C} \quad (2)$$

where $K_1 = 2.4$.

Alternatively, the $\bar{d}$ of 2D brushes (chains per μm^2 GO backbone, $\bar{d}_2$) can be calculated from the equation

$$\bar{d}_2 = \frac{M_C}{M_P}\frac{W_P}{\frac{W_C}{2} \times 2 \times A_b \times 10^{-8}} = \frac{M_C \times 10^8}{M_P \times A_b}\frac{W_P}{W_C} \quad (3)$$

where A_b represents the area of a benzene ring in graphene (5.24 $Å^2$). So eq 3 can also be modified as

$$\bar{d}_2 = K_2\frac{W_P}{W_C} \quad (4)$$

Herein $K_2 = 4.58 \times 10^3$. Notably, the polymer arms are anchored on both sides of GO, so $\bar{d}_2$ means the average arm density on a single side.

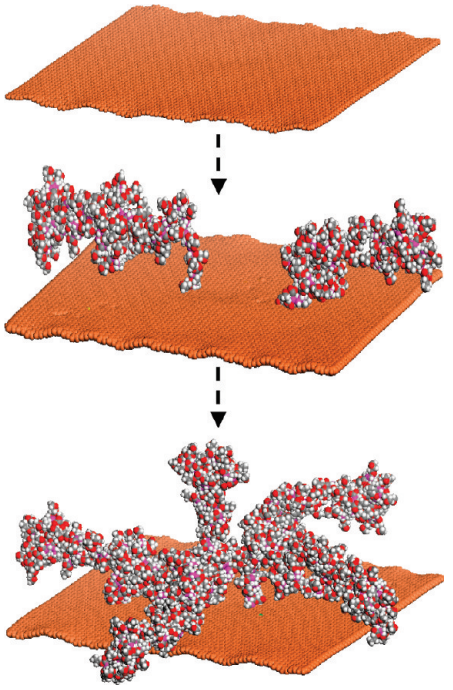

Figure 3. Cartoon pictures for the growing process of a cluster of PGMA chains (the degree of polymerization is 100) on a graphene sheet (made by Materials Studio software 4.0).

Consequently, to calculate the grafted arm density, W_C and W_P should be measured at first. Generally, W_C and W_P can be readily obtained from the TGA curves of brushes because the grafted polymer has a weight loss stage below 550 °C, and the residual weight fraction above 550 °C is assigned to W_C. The calculated $\bar{d}$ values are listed in Table 1 and plotted in Figure 2b. In order to evaluate the accuracy of the calculated density, we could deduce the specific surface area (S) of graphene as 2628.5 m^2/g from the final value of brush density ($S = (2W_pN_A)/(W_CM\bar{d}_2)$, where N_A represents the Avogadro constant, 6.02×10^{23}). Our deduced S is almost equal to the value reported in the literature (2630 m^2/g).[45]

As illustrated in Figure 2b, the $\bar{d}$ increases dramatically and almost linearly within the first 10 h, and relatively slowly after 18 h, and eventually reaches 15 960 chains per μm^2 of single side of GO at 48 h. Notably, from the AFM images, we can see that the $\bar{h}$ also increases from 1.7 to 12.8 nm with the reaction time, which is not resulted from the enlarging or growing of polymer arms since the propagation of a chain stopped rapidly after initiating but from the augmenting of grafting density. At a low density, the anchored arms could lie down or collapse on the sheet backbone for the van der Waals interactions; at a high density, the arms, especially those close to the center of polymer clusters, would stand up erectly due to the steric repulsion with each other, and the higher the density, the stronger the force, the longer the stretch of arms, the greater the height would be. From the increasing tendency of $\bar{d}$ and $\bar{h}$, we can speculate their relationship: $\bar{h} = k\bar{d}^{\alpha}$ for GO-*g*-PGMA brushes (herein $\alpha \approx 1$). The brush growing process can be depicted with cartoon pictures as shown in Figure 3.

Even though the fraction of grafted polymer (~80 wt %) is fairly high, the arm density on graphene oxide is obviously lower than that of CNTs-based polymer brushes or other surface brushes that were prepared by the "grafting from" approach.[41,46] This is mainly because our synthesis method basically belongs to a grafting to process. Another reason is

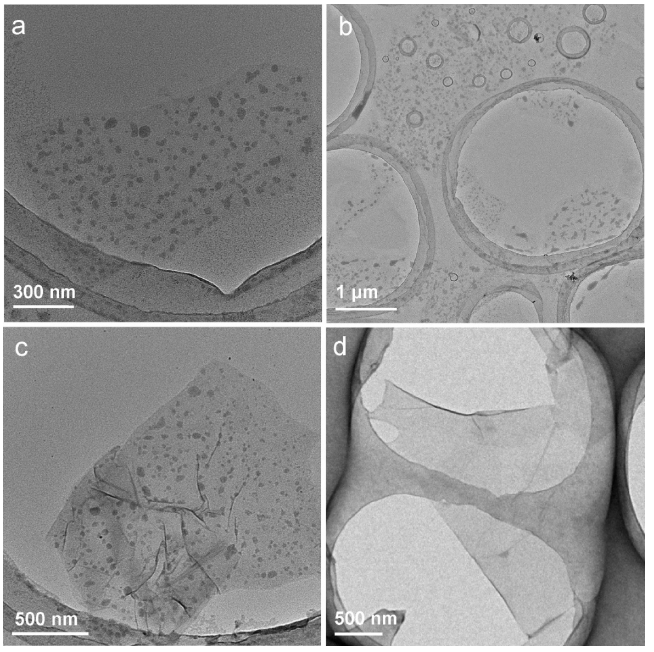

Figure 4. Representative TEM images of GO-*g*-PGMA (a, b), G-*g*-PGMA (c), and pristine GO (d).

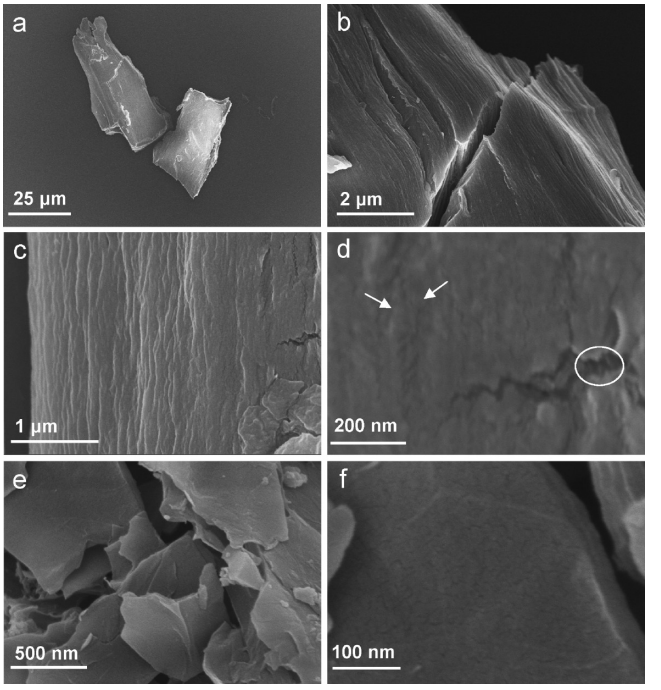

Figure 5. SEM images of bulk samples of GO-*g*-PGMA (a−d) and GO-*g*-PS (e, f) with the ratio of monomer to initiator 200:1 after centrifugal washing and vacuum drying, respectively.

that the molecular weight of grafted polymer arms is quite high. The strong steric hindrance associated with high molar mass of polymeric radicals is unfavorable to the high density grafting. Nevertheless, such a grafting density is comparable to that of previously reported "grafting to" cases on graphene (e.g., 1 chain of polystyrene with M_n 2500 g/mol per 980 carbon atoms).[47] In addition, the final $\overline{d}$ value is higher than the density of the elastic hairs or setae, including their end spatulae on a gecko foot by about at least 3 orders of magnitude, and also higher than the reported highest density of biomimic gecko foot, aligned carbon nanotubes array,[48] by about at least 2 orders of magnitude, indicating the possible biomimic applications of such soluble giant 2D molecular brushes.

Besides the window of time, we also tried to adjust the grafted arms by changing the feed ratio of monomer to initiator (R_{feed}) that may alter the molar mass of polymers to some extent. The results showed that the amount of arms could be slightly modulated (Figure 2 and Figure S13c), suggesting the flexibility of the synthesis strategy (Figures S14−S17). For instance, when R_{feed}s were changed to 50/1 and 1000/1 for cases of GO-*g*-PGMA, the grafted polymer contents approached 83.0 and 91.6 wt %, respectively, showing that the amount of arms increased with augmenting the R_{feed}. Moreover, we performed tens of experiments to repeat the experiments with different GO scales from tens of milligram to several grams, obtaining similar results to those mentioned above, revealing the good reproducibility of the presented synthesis strategy.

TEM and SEM Observations of 2D Molecular Brushes. The sheet structure and morphology of 2D molecular brushes of GO-*g*-PGMA were also observed and confirmed by TEM and SEM measurements. The representative TEM image (Figure 4a) shows a monolayer GO sheet attached with tufts of polymer protuberances that are evenly dispersed on the whole sheet. Under the low-magnitude image (Figure 4b), many individual sheets are observed, and each GO sheet has been evenly decorated with polymer clusters. As a comparison, no such kind of protuberances can be detected for the pristine GO sheets (Figure 4d). These results further indicate that the polymer chains have been successfully grafted on GO sheets through the *in situ* radical polymerization approach.

Figure 5 shows the typical surface morphology of the dried GO-*g*-polymer brushes. Well-packed layers are observed for the sample obtained by centrifugal washing at a low magnification (Figure 5a,b). From detailed observations, we can find that each layer is equipped with a shaggy surface (Figure 5c). The high-resolution SEM image shows that the flat surface is coated with a rough polymer layer (Figure 5d, marked by the arrows for a clear view). Furthermore, relatively blunt and coarse edges can be observed from the fracture (Figure 5d, marked by a circle).

Obviously, the observations of TEM and SEM are in agreement with the AFM visualizations, validating the successful synthesis of 2D molecular brushes.

Extension of the Synthesis Strategy. The above PGMA cases have sufficiently shown the feasibility, simplicity, and reproducibility of our synthesis strategy, paving the way for facile, large-scale production of individually dispersible 2D molecular brushes. To demonstrate the generality of our strategy, we conducted hundreds of experiments to extend it to all vinyl monomers available for us including acrylates (e.g., methyl acrylate (MA), hydroxyethyl acrylate (HEA), and acrylic acid (AA)), methacrylates (e.g., methyl methacrylate (MMA), butyl methacrylate (BMA), *tert*-butyl acrylate (*t*-BA), hydroxyethyl methacrylate (HEMA), 2-(dimethylamino)ethyl methacrylate (DMA), and methacrylic acid (MAA)), styrenics (styrene (St), and sodium *p*-styrenesulfonate (SSNa)), acrylamides (acrylamide (AM), and *N*-isopropylacrylamide (NIPAAm)), and 4-vinylpyridine (VP) (see Scheme 1). We got the unbelievable success for all cases, and obtained various 2D macromolecular brushes of polymer-grafted GO covering from polar to apolar, water-soluble to oil soluble, acidic to basic, and from functional to common polymers (Figures S18−S21 and Table S2).

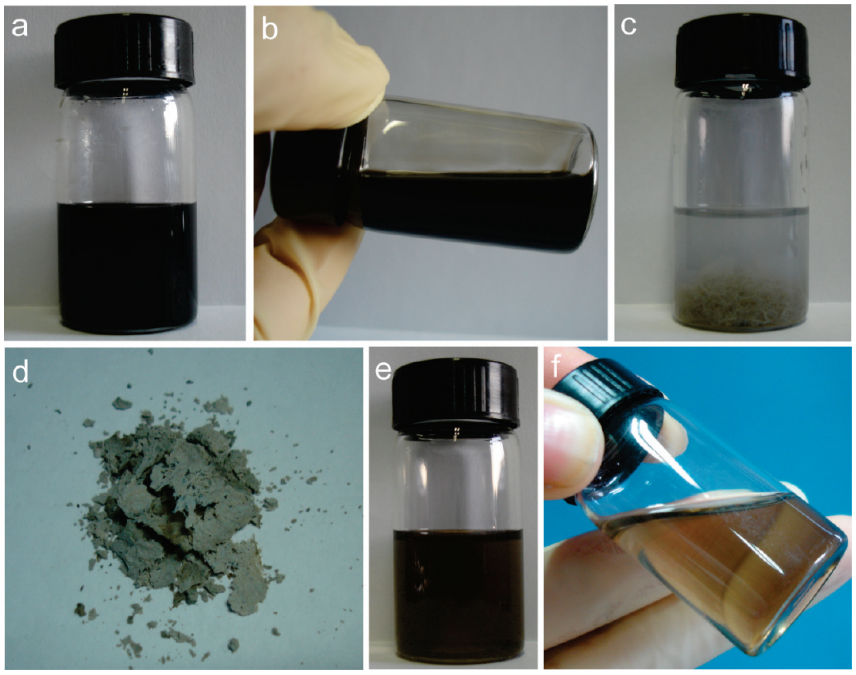

Figure 6. (a) Solution obtained after polymerization of GMA in the presence of GO for 48 h, and the vial was placed statically for around 2 months. (b) No sediment was observed at the bottom of the vial, indicating the "true solution" character for the dispersions. (c) The solution was precipitated by adding it into methanol. (d) Dried solid collected from (c). The solid in (d) was redissolved in DMF (e, f) with different background color, showing the superb solubility of the solid composite.

Additional typical SEM images of GO-*g*-PS are displayed in Figure 5e,f, clearly presenting sheet surfaces coated with dense brush clusters. The functional polymer-grafted GO brushes with pH, ion, salt, or temperature-stimuli responsive properties promise their great potentials in both academic and application fields, which will be reported later.

In addition, chemically reduced graphene sheets were also utilized as backbones to synthesize 2D brushes. TEM observations also show the similar structure to that of GO cases: hairy polymer clusters are evenly grafted on graphene backbones (Figure 4c). TGA curves and AFM images of polymer-grafted graphene are shown in Figure S22.

Properties of 2D Molecular Brushes and Their Composite. Notably, even through the amount of grafted polymer is relatively high, the fraction of grafted polymer compared to the free polymer is quite small (~2%). Regarding the potential application of the products and the high fraction of free polymers, we think that our approach can be used directly to produce nanocomposite of polymer-grafted GO and (free) polymer because of their good compatibility. As seen in Figure 6, the resulting solution after polymerization was homogenously black solution without any sediment after placing statically for 2 months (Figure 6a,b). After addition of methanol as precipitator to the solution, gray sediment appeared without any separately black granules (Figure 6c); after drying, we got pure gray solids (Figure 6d). This indicates that the GO-based brushes were well dispersed in polymer matrix. The dried solid can be well soluble in solvents again (Figure 6e,f). These results suggest that nanocomposite of polymer-grafted GO and (free) polymer can be readily prepared by the solution-processing technique. The application studies on such compatible composites are still in progress.

After efficient washing and centrifugation, neat polymer-grafted GO was obtained. A series of solvents were utilized to test the solubility of the resulting 2D molecular brushes, and parts of results are shown in Figure 7 as photographs. According to the nature of grafted arms, each kind of brush can be solubilized in selected solvents from the horizontal point of view; for a required solvent, corresponding soluble macromolecular brushes can be selected from the vertical point of view.

As mentioned above, after polymerization, the GO backbones were basically reduced (Figure S11). We further reduced the GO backbones by $N_2H_4 \cdot H_2O$[40] and found that the reduced 2D brushes of G-*g*-polymer preserved their morphology and solubility. This brings a significant progress to the process of such novel macromolecular brushes and GO/graphene-based polymer composites since pristine graphene and GO have very limited solubility in most of solvents.

It is noteworthy that GO-*g*-PGMA macromolecules show a very low intrinsic viscosity in DMF solution (~100 mL/g). This viscosity value is much lower than that of pristine GO dispersion (~780 mL/g) and close to the value of a common linear polymer such as polystyrene with 10^5 scale molar mass, indicating that the 2D molecular brushes have hardly intermolecular chain entanglements. This is similar to the globular macromolecules such as dendritic polymers.[49] This property probably enables the 2D brushes useful as nanofillers to improve the processability and performance of common polymers.

Because of their good solubility, the resulting 2D brushes can be readily coated homogeneously on solid substrates to form desired coating by direct painting (Figure 8a) as well as processed into self-standing films by solution casting (Figure 8b). Interestingly, the films of G-*g*-PGMA show the polymer content-dependent conductivity: 6×10^{-1} S/cm for reduced graphene, 6.5×10^{-2} S/cm for brushes at 24 h, and 8.4×10^{-3} S/cm at 48 h.[47,50,51] The highly processable 2D brushes could be used directly as building blocks to easily fabricate large-area surface brushes by solution casting or coating for biomimetic water-based lubrication, friction

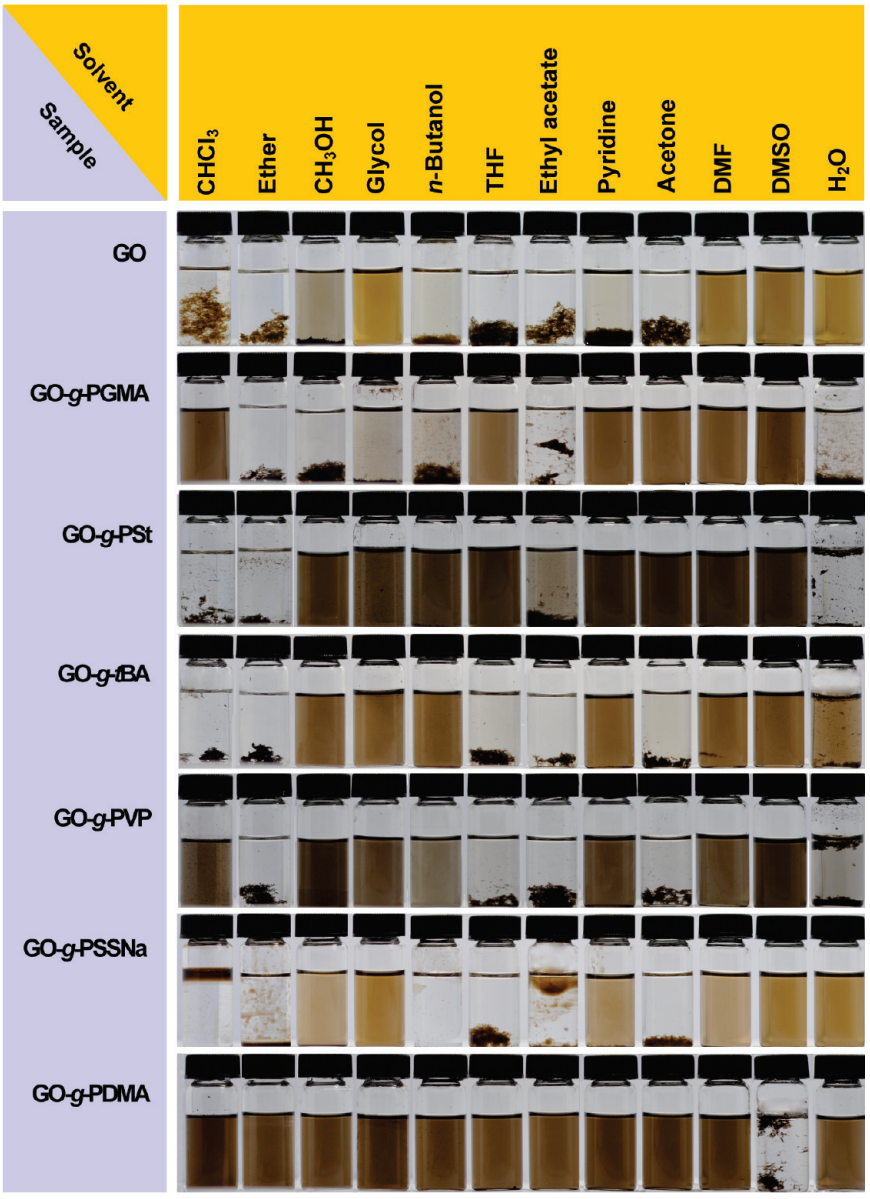

Figure 7. Photographs of GO and GO-*g*-polymer 2D macromolecular brushes placed in various solvents.

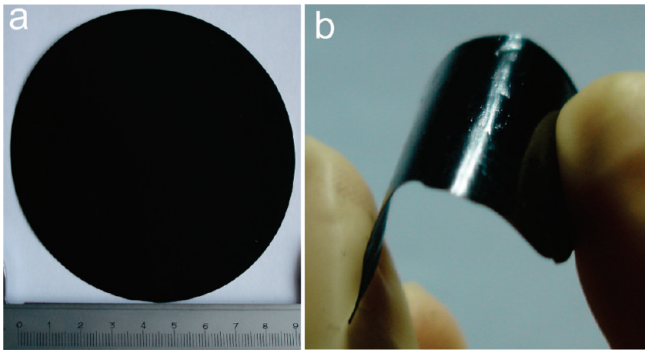

Figure 8. (a) Photograph of GO-*g*-PGMA coated on a nylon filter paper. (b) Self-standing film of pure GO-*g*-PGMA macromolecular brushes made by solution casting.

decreasing, and electrical conducting. Moreover, the numerous functional groups of brushes promise their use of molecular carriers to load guest matters and construct desired structures and composites.

Conclusions

In summary, we have developed a facile, powerful, reliable, and general strategy for scalable synthesis of GO/graphene-based 2D molecular brushes, a novel kind of giant molecules with sheet topology, laying the foundation for large-scale production of such giant macromolecules. The combination of high solubility, low viscosity, good processability, tunable electrical conductivity, and visible micrometer-scale sheet structures makes the 2D molecular brushes promising in a wide applications covering from biomimetic coatings to nanocomposites. Moreover, graphene or GO could be used as a novel kind of nanotable for the direct observation of molecular growth, polymerization kinetics, chemical reactions, and morphology of polymers and biomacromolecules, which would put a big forward for chemistry and biology. Other properties including rheology and viscoelastics of the 2D molecular brushes are currently investigated and explored.

Acknowledgment. This work was financially supported by the National Natural Science Foundation of China (No. 50773038 and No. 20974093), National Basic Research Program

of China (973 Program) (No. 2007CB936000), the Fundamental Research Funds for the Central Universities (2009QNA4040), Qianjiang Talent Foundation of Zhejiang Province (2010R10021), and the Foundation for the Author of National Excellent Doctoral Dissertation of China (No. 200527). The authors are grateful to Prof. Jinwen Qian for the help of viscosity measurements.

Supporting Information Available: Additional AFM images of 2D molecular brushes, ^{1}H NMR spectra, TGA curves, DSC curves, and XRD patterns. This material is available free of charge via the Internet at http://pubs.acs.org.

References and Notes

(1) Lee, S.; Spencer, N. D. *Science* **2008**, *319*, 575–576.
(2) Raviv, U.; Giasson, S.; Kampf, N.; Gohy, J.; JérÔme., R.; Klein, J. *Nature* **2003**, *425*, 163–165.
(3) Ryu, D. Y.; Shin, K.; Drockenmuller, E.; Hawker, C. J.; Russell, T. P. *Science* **2005**, *308*, 236–239.
(4) Klein, J. *Science* **2009**, *323*, 47–48.
(5) Klein, J.; Kumacheva, E.; Mahalu, D.; Perahia, D.; Fetters, L. J. *Nature* **1994**, *370*, 634–636.
(6) Zhang, M. F.; Müller, A. H. E. *J. Polym. Sci., Part A: Polym. Chem.* **2005**, *43*, 3461–3481.
(7) Sheiko, S. S.; Sumerlin, B. S.; Matyjaszewski, K. *Prog. Polym. Sci.* **2008**, *33*, 759–785.
(8) Schappacher, M.; Deffieux, A. *Science* **2008**, *319*, 1512–1515.
(9) Mansky, P.; Liu, Y.; Huang, E.; Russell, T. P.; Hawker, C. *Science* **1997**, *275*, 1458–1460.
(10) Milner, S. T. *Science* **1991**, *251*, 905–914.
(11) Edmondson, S.; Osborne, V. L.; Huck, W. T. S. *Chem. Soc. Rev.* **2004**, *33*, 14–22.
(12) Zhao, B.; Brittain, W. J. *Prog. Polym. Sci.* **2000**, *25*, 677–710.
(13) Klein, J.; Kumacheva, E.; Perahia, D.; Fetters, L. J. *Acta Polym.* **1998**, *49*, 617–625.
(14) Raviv, U.; Frey, J.; Sak, R.; Laurat, P.; Tadmor, R.; Klein, J. *Langmuir* **2002**, *18*, 7482–7495.
(15) Kobayashi, M.; Terayama, Y.; Hosaka, N.; Kaido, M.; Suzuki, A.; Yamada, N.; Torikai, N.; Ishihara, K.; Takahara, A. *Soft Matter* **2007**, *3*, 740–746.
(16) Drobek, T.; Spencer, D. *Langmuir* **2008**, *24*, 1484–1488.
(17) Subbotin, A.; Jong, J. D.; Brinke, G. T. *Eur. Phys. J. E* **2006**, *20*, 99–108.
(18) Geim, A. K.; Novoselov, K. S. *Nature Mater.* **2007**, *6*, 183–191.
(19) Geim, A. K. *Science* **2009**, *324*, 1530–1534.
(20) Ruoff, R. S. *Nature Nanotechnol.* **2008**, *3*, 10–11.
(21) Dikin, D. A.; Stankovich, S.; Zimney, E. J.; Piner, R. D.; Dommett, G. H. B.; Evmenenko, G.; Nguyen, S. T.; Ruoff, S. R. *Nature* **2007**, *448*, 457–460.
(22) Mkhoyan, K. A.; Contryman, A. W.; Silcox, J.; Stewart, D. A.; Eda, G.; Mattevi, C.; Miller, S.; Chhowalla, M. *Nano Lett.* **2009**, *9*, 1058–1063.
(23) Kudin, K. N.; Ozbas, B.; Schniepp, H. C.; Prud'homme, R. K.; Aksay, L. A. *Nano Lett.* **2008**, *8*, 36–41.
(24) (a) Fang, M.; Wang, K.; Lu, H.; Yang, Y.; Nutt, S. *J. Mater. Chem.* **2010**, *20*, 1982–1992. (b) Fang, M.; Wang, K. G.; Lu, H. B.; Yang, Y. L.; Nutt, S. *J. Mater. Chem.* **2009**, *19*, 7098–7105.
(25) (a) Stankovich, S.; Piner, R. D.; Chen, X. Q.; Wu, N. Q.; Nguyen, S. T.; Ruoff, R. S. *J. Mater. Chem.* **2006**, *16*, 155–158. (b) Lee, S. H.; Dreyer, D. R.; An, J.; Velamakanni, A.; Piner, R. D.; Park, S.; Zhu, Y.; Kim, S. O.; Bielawski, C. W.; Ruoff, R. S. *Macromol. Rapid Commun.* **2010**, *31*, 281–288.
(26) Shen, J. F.; Hu, Y. Z.; Li, C.; Qin, C.; Ye, M. X. *Small* **2009**, *5*, 82–85.
(27) Veca, L. M.; Lu, F. S.; Meziani, M. J.; Cao, L.; Zhang, P. Y.; Qi, G.; Qu, L. W.; Shrestha, M.; Sun, Y. P. *Chem. Commun.* **2009**, 2565–2567.
(28) (a) Kim, H.; Abdala, A. A.; Macosko, C. W. *Macromolecules* **2010**, *43*, 6515–6530. (b) He, H.; Gao, C. *ACS Appl. Mater. Interfaces* **2010**, *2*, 3201–3210. (c) Kou, L.; He, H.; Gao, C. *Nano-Micro Lett.* **2010**, *2*, 177–183. (d) Han, J.; Gao, C. *Nano-Micro Lett.* **2010**, *2*, 213–226.
(29) Xu, Z.; Gao, C. *Macromolecules* **2010**, *43*, 6716–6723.
(30) Dreyer, D. R.; Park, S.; Bielawski, C. W.; Ruoff, R. S. *Chem. Soc. Rev.* **2010**, *39*, 228–240.
(31) Li, D.; Müller, M. B.; Gilje, S.; Kaner, R. B.; Wallace, G. G. *Nature Nanotechnol.* **2008**, *3*, 101–105.
(32) Tung, V. C.; Allen, M. J.; Yang, Y.; Kaner, R. B. *Nature Nanotechnol.* **2009**, *4*, 25–29.
(33) Hummers, W. S.; Offeman, R. E. *J. Am. Chem. Soc.* **1958**, *80*, 1339–1339.
(34) Shaffer, M. S. P.; Koziol, K. *Chem. Commun.* **2002**, 2074–2075.
(35) Qin, S. H.; Qin, D. Q.; Ford, W. T.; Herrera, J. E.; Resasco, D. E.; Bachilo, S. M.; Weisman, R. B. *Macromolecules* **2004**, *37*, 3965–3967.
(36) Qin, S. H.; Qin, D. Q.; Ford, W. T.; Herrera, J. E.; Resasco, D. E. *Macromolecules* **2004**, *37*, 9963–9967.
(37) Samulski, E. T.; Desimone, J. M.; Jr, M. O. H.; Menceloglu, Y. Z.; Jarnagin, R. C.; York, G. A.; Labat, K. B.; Wang, H. *Chem. Mater.* **1992**, *4*, 1153–1157.
(38) Jeon, H. J.; Youk, J. H.; Yu, W. R. *Macromol. Res.* **2010**, *18*, 458–462.
(39) Flory, P. J. *Principles of Polymer Chemistry*; Cornell University Press: Ithaca, NY, 1953.
(40) Park, S.; Ruoff, R. S. *Nature Nanotechnol.* **2009**, *4*, 217–224.
(41) (a) Kong, H.; Gao, C.; Yan, D. Y. *J. Am. Chem. Soc.* **2004**, *126*, 412–413. (b) Kong, H.; Gao, C.; Yan, D. *Macromolecules* **2004**, *37*, 4022–4030. (c) Gao, C.; Muthukrishnan, S.; Li, W. W.; Yuan, J. Y.; Xu, Y. Y.; Muller, A. X. E. *Macromolecules* **2007**, *40*, 1803–1815.
(42) Gao, W.; Alemany, L. B.; Ci, L.; Ajayan, P. M. *Nature Chem.* **2009**, *1*, 403–408.
(43) Ramanathan, T.; Abdala, A. A.; Stankovich, S.; Dikin, D. A.; Herrera-Alonso, M.; Piner, R. D.; Adamson, D. H.; Schniepp, H. C.; Chen, X.; Ruoff, R. S. *Nature Nanotechnol.* **2008**, *3*, 327–331.
(44) Gao, C.; Vo, C. D.; Jin, Y. Z.; Li, W. W.; Armes, S. P. *Macromolecules* **2005**, *38*, 8634–8648.
(45) Stoller, M. D.; Park, S. J.; Zhu, Y. W.; An, J.; Ruoff, R. S. *Nano Lett.* **2008**, *8*, 3498–3502.
(46) (a) Ohno, K.; Kon, K.; Tsujii, Y.; Da, T. *Macromolecules* **2002**, *35*, 8989–8993. (b) Ohno, K.; Morinaga, T.; Kon, K.; Tsujii, Y.; Da, T. *Macromolecules* **2005**, *38*, 2137–2142.
(47) He, H. K.; Gao, C. *Chem. Mater.* **2010**, *22*, 5054–5064.
(48) Qu, L. T.; Dai, L. M.; Stone, M.; Xia, Z. H.; Wang, Z. L. *Science* **2008**, *322*, 238–242.
(49) Gao, C.; Yan, D. *Prog. Polym. Sci.* **2004**, *29*, 183–275.
(50) Stankovich, S.; Dikin, D. A.; Dommett, G. H. B.; Kohlhaas, K. M.; Zimney, E. J.; Stach, E. A.; Piner, R. D.; Nguyen, S. T.; Ruoff, R. S. *Nature* **2006**, *442*, 282–286.
(51) Rivadulla, F.; Mateo-Mateo, C.; Correa-Duarte, M. A. *J. Am. Chem. Soc.* **2010**, *132*, 3751–3755.